Uotinen, Lauri; Korpi, Eero; Hartikainen, Ari; Yorke, Raphael; Antikainen, Juha; Johansson, Fredrik; Rinne, Mikael

A method to downscale joint surface roughness and to create replica series using 3D printed molds

Published in:
ISRM 13th International Congress on Rock Mechanics, Montreal, May 10-13, 2015

Published: 01/01/2017

Document Version
Peer-reviewed accepted author manuscript, also known as Final accepted manuscript or Post-print

Please cite the original version:
Uotinen, L., Korpi, E., Hartikainen, A., Yorke, R., Antikainen, J., Johansson, F., & Rinne, M. (2017). A method to downscale joint surface roughness and to create replica series using 3D printed molds. In *ISRM 13th International Congress on Rock Mechanics, Montreal, May 10-13, 2015* Canadian Institute of Mining, Metallurgy and Petroleum.

A METHOD TO DOWNSCALE JOINT SURFACE ROUGHNESS AND TO CREATE REPLICA SERIES USING 3D PRINTED MOLDS

*L. K. T. Uotinen, E. Korpi, A. Hartikainen, R. Yorke, J. Antikainen
Aalto University
Espoo, Finland
*(*Corresponding author: lauri.uotinen@aalto.fi)*

F. Johansson
KTH Royal Institute of Technology
Stockholm, Sweden

M. Rinne
Aalto University
Espoo, Finland

A METHOD TO DOWNSCALE JOINT SURFACE ROUGHNESS AND TO CREATE REPLICA SERIES USING 3D PRINTED MOLDS

ABSTRACT

In order to determine the in-situ shear strength of rock joints, large scale testing is required. However, this is both expensive and difficult to execute. One possible method to overcome this may be to use photogrammetry to capture large joint surface roughness in-situ and downscale it to replica samples, which could be sheared in laboratory. In this paper, as a first part in such a method, a technique to digitize surface roughness and to produce replica samples for laboratory shear testing from a larger joint sample are presented. First, a thin granitic rock slice with dimensions of 1.75 m x 0.95 m of granitic intact rock was chosen for the study. The joint surface is fresh and created through tensile induced splitting. The large joint sample is digitized using photogrammetry. Then, one full-scale 1.7 m x 0.6 m geometry is cropped from the digitized joint geometry and then subsamples at 10x, 7.5x, 5x, 2.5x and 1x scales. All sub-geometries are scaled down digitally to produce 0.17 m by 0.06 m geometries. The geometries are used to make casting molds both positive and negative to produce samples with perfect matedness. The casting molds are 3D printed in polylactic acid plastic and C60/75 concrete is cast to produce a replica series. In addition to the creation of this replica series, two pilot replicas are also tested using a portable shear box with a 0.5 MPa normal pressure. The results from the pilot rounds are presented and discussed. Finally, suggestions for future research are given.

KEYWORDS

Joint, Crack, Fracture, Photogrammetry, 3D printing, Replica, Concrete, Shear Box

INTRODUCTION

The rock mass strength is in many cases controlled by the shear strength of rock joints, especially in hard rock masses. The shear strength is generally found to be influenced by several parameters, including normal stress, the basic friction angle of the intact rock, the joint surface roughness, the joint wall compressive strength, the matedness of the joint surfaces, weathering and infilling. The effect of these parameters for the joint shear strength can be evaluated in laboratory scale. However, the shear strength is known to be scale dependent. How the scale effect influences the strength is not fully understood. The general consensus is that the shear strength decreases when sample size increases, i.e. a negative scale effect (Bandis et al. 1981). However, some studies have presented contradictory results, see for example Hencher et al. (1993) and Kutter & Otto (1990). The extent and nature of the scale effect is still a question of debate (Tatone & Grasselli 2013).

The difficulty of defining the design scale values for the rock joint parameters is the lack of robust and affordable testing methods for design scale rock joints. Testing large and heavy in-situ samples requires massive and expensive testing and transport equipment. Secondly, the representativeness of results is questionable when defining the parameters using laboratory scale tests. The overall aim of this research project aims to develop a method to evaluate design scale rock parameters using small scale laboratory tests. As a first part of such a method, a technique, where the rock joint surface geometry is captured using photogrammetry and digitally downscaled to the laboratory testing scale has been developed. This geometry is then converted into a 3D surface negative casting mold and the samples are replicated using high-strength concrete. The replica samples are tested using a portable shear box. The method allows testing the same joint surface geometry at different scales. Previously, this type of studies, such as Barton & Choubey (1977), has been performed using in-situ shear tests. Large samples have first been tested. After that, samples have been sawn into smaller parts and these parts have been re-tested. Compared to earlier studies, the benefit of

our method being under development is that samples with different sizes can be tested with no abrasion from previous shear tests. Another benefit is that several replica copies of the same joint geometry may be made and tested to reduce the scatter of results. A limitation of the presented methodology is that small scale roughness will be lost during the downscaling. How to account for this limitation will be analyzed in future studies and has not been considered in this paper.

This paper describes the replication method we have developed. First we introduce how the source geometry was obtained, describe the photogrammetric process, production of the point cloud and transforming it into a printable 3D solid. Then the casting process and the resulting quality are described. Finally pilot round results are shown and discussed. The replica campaign is taking place during autumn 2014 and the results will be published separately.

METHODS

Sample acquisition

The rock slab (Figure 1) used as rock joint source geometry for photogrammetry was split from a larger boulder before it was delivered to Myrskylä, Finland. The splitting was performed using approximately 10 cm long wedges at the one side of the boulder with 10 - 15 cm distance. The slab had been sawn to approximately 3 cm thick plate including the split surface from the side of the boulder to produce smooth surface. The granitic rock surface had a size of approximately 175 cm x 95 cm (1.84:1). The rock had been outside few months between sawing and photographing. It is possible that frost might have caused some damage to the surface if this storage period has included periods with the temperature below 0° C. However, the storage period can be considered relatively short. Therefore, possible damages are presumably very small and the surface can be considered fresh. There are some localized damaged areas with visible damage (as seen in white in Figure 1) and the sampling pattern was designed to avoid these regions, but they are included in the larger subgeometries. The surface was cleaned before photographing to remove any dust and dirt from transportation and storage period.

Figure 1. The granitic rock surface with dimensions of 175 cm x 95 cm resting on a pallet


Figure 2. The 414 camera positions used in photographing of the thin rock slab

Photogrammetry

The photographs were taken using a Canon EOS 600D DSLR camera and a Canon EF 35mm f/2 IS USM objective. The rock was placed outdoors to a shady location to prevent bright reflections from the glossy minerals. The aperture was set to f/11, exposure time to 1/60 seconds and ISO value to 100. A folding rule was placed on the edge of the rock to provide a reference measure of the rock.

A total of 414 photos were taken from different angles (Figure 2). Most photos were taken at close range with small translation movements and large overlaps. Between series the camera angle was changed. The camera angle was varied vertically (pitch) from 30 to 80 degrees and horizontally (yaw) from -45 to 45 degrees and some of the pictures were taken at different sensor angle (roll) from 0 to 45 degrees to reduce sensor bias. In the end of the shoot, some images were taken at longer distances up to 4 m away to include the whole slab in a single image.

Point cloud processing

The data processing starts with creating a point cloud from the photographs. The VisualSFM 0.5.25 software is used to form the point cloud. First, the matching of same points in different pictures is performed. Then 3D positions are calculated for point matches in a relative coordinate system. This function forms a sparse reconstruction, which is the preliminary stage for the dense reconstruction. The dense reconstruction is calculated and the point cloud is saved in PLY (polygon file format). The resulting point cloud is presented in the Figure 3.

Next, the Cloud Compare 2.5.5.2 software is used to segment out the unused parts of the point cloud. The point cloud after the segmentation is presented in Figure 4. In addition to the points outside of the rock, some compromised parts of the rock are removed. These parts of the rock include half-barrels, cracks and undulation induced by the splitting process. These regions were left out to obtain a rock surface, which can be considered representative to a natural fresh rock joint. The information about the reference measure (folding rule) was used to scale the point cloud to the correct size.

Figure 3. The entire point cloud in Cloud Compare software (27 million points)

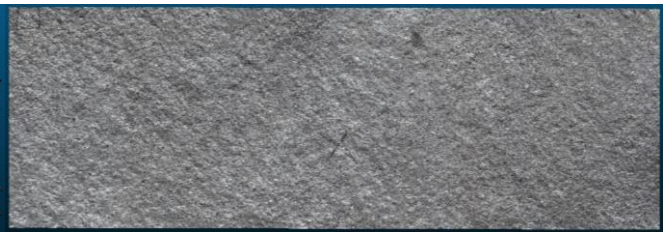

Figure 4. Point cloud after removal of unused parts (16 million points, 1700 mm x 600 mm)

After the removal of unused and compromised parts and scaling, the size of the cloud is 1.7 m x 0.6 m and it contains 16548045 points. The point density of the cloud is 16.2 points / mm^2. Next, the cloud is rotated and translated (Girardeau-Montaut 2012a) to xy–plane with principal component analysis procedure (Dimitrov 2008). To form a mesh from the point cloud, 2D–Delaunay triangulation (Delaunay 1934) is calculated for the projection on the xy–plane with Delaunay 2D (best LS plane) (Girardeau-Montaut 2012b). The generated 3D–mesh is saved to a file using the STL (Standard Tessellation Language) ASCII text format.

Table 1. Sampling pattern

Identifier	Quantity	Source geometry size	Sampling location
10x1	1	1700 mm x 600 mm	center point
7.5x2-5	4	1275 mm x 450 mm	corners[a]
5x6-9	4	850 mm x 300 mm	quarters
2.5x10-13	4	425 mm x 150 mm	quarters
1x14-17	4	170 mm x 60 mm	quarters

[a] the 7.5x series reuses portions of the slab effectively weighting the central regions

Before calculating the meshes for the sub-geometries, the cropping has to be performed to the point cloud to sample parts of the point. The target size to be tested in the portable shear box is 170 mm x 60 mm. The source geometry will be sampled at different sizes (10x, 7.5x, 5x, 2.5x and 1x) according to the sampling pattern shown in Table 1. After cropping each geometry will be scaled down to the target size. Figure 5 illustrates the sampling locations. It should be noted that the 7.5x geometry oversamples the geometry effectively weighting the slab central regions. The 2.5x and 1x series undersample the geometry, which may cause a representability problem as a part of the slab geometry

is not tested at these scales. Scales 10x, 5x and 1x form the primary testing series, which is then augmented by the supplementary testing series of 7.5x and 2.5x.

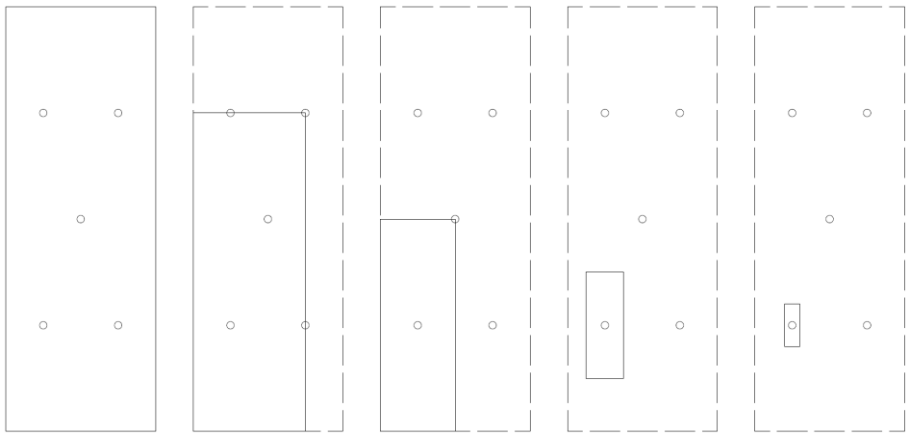

Figure 5. The cropping pattern 10x, 7.5x, 5.0x, 2.5x, 1x center and quarter points noted with circles

The point cloud was too dense for conventional modelling software to handle and a custom Python 2.7.5 script was created. The steps taken by the script are illustrated in Figure 6. The script first reads the STL ASCII format mesh and then creates a solid by finding the convex hull, the perimeter of the Delaunay triangulation. The script creates a collar for the mesh plane by expanding convex hull points outward to the assigned collar frame. This forms the variable angle θ ($0° < \theta < 90°$) between the collar frame and the convex hull points. The trapezoids between collar frame and convex hull are triangulated with two triangles excluding trapezoids containing corner points. The corners are triangulated with three triangles that include corner point as the divider. Bottom frame is created from the collar frame by copying it perpendicularly to the assigned depth. The sides are triangulated with two triangles for every trapezoid. The bottom plane is triangulated with a 2D–Delaunay network. The counterpart–model is created by inserting a negative depth value, which reverses the direction. The script creates a new STL ASCII format file, which contains the generated solid. After this, the STL file can be opened in a slicing software to create the tool head code for the 3D printing. The final version of the printed mold using this method is shown in Figure 7. The final sample has 5 mm margins (the collar) and is 180 mm x 70 mm x 10 mm with 170 mm x 60 mm of active joint surface. The margin slopes reduce the tensile failure near the outer perimeter, which was detected in early piloting rounds.

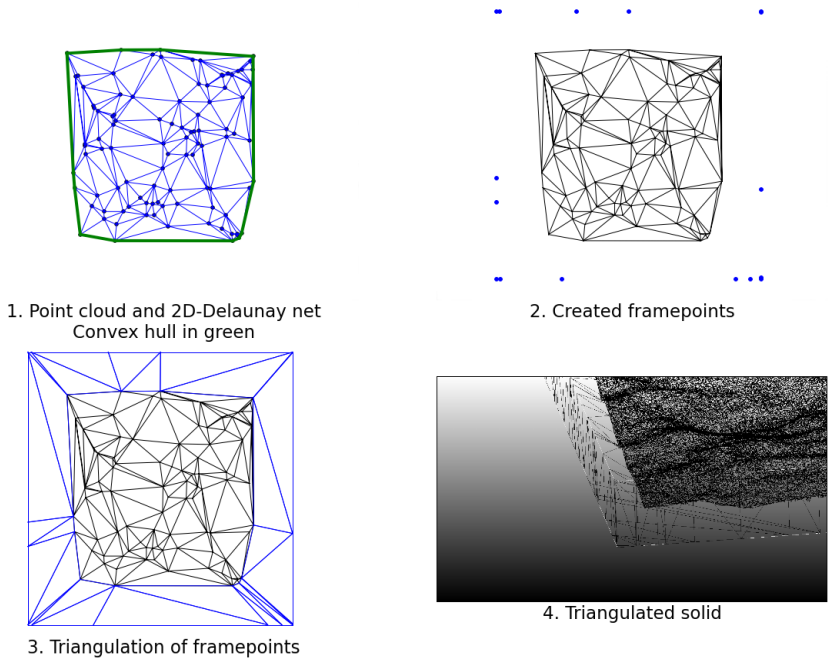

Figure 6. The steps performed in the solid generation Python script

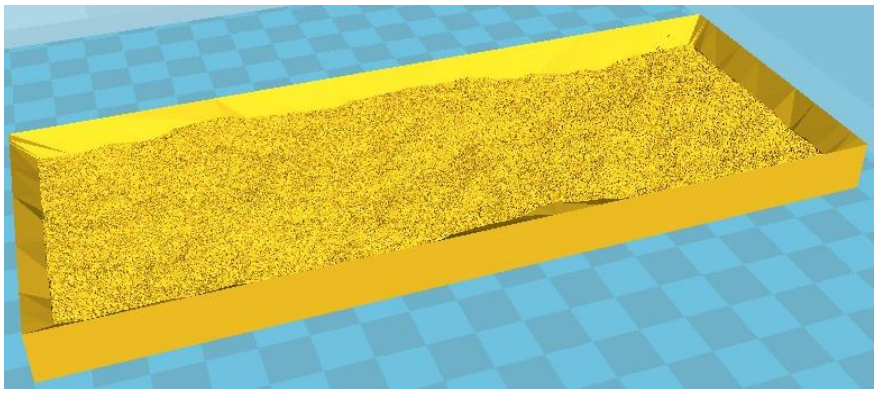

Figure 7. The printable part of the casting mold assembly

Casting mold production

The surface casting molds were printed either using Ultimaker Original v3 2013 or Ultimaker^2 2014 fast prototyping fused filament fabrication 3D printers. The used slicing software (Cura 14.07) settings are shown in Table 2. After printing, the surfaces are inspected and any anomalies (such as thin hairs caused by oozing during travel moves) are removed.

Table 2. 3D printing settings used in mold production

Parameter	Value	Notes
layer height	0.050 mm	20 layers per mm
shell thickness	1.000 mm	perimeter
bottom/top thickness	1.000 mm	
fill density	20 %	rectilinear
print speed	50 mm/s	
nozzle temperature	215 C	for polylactic acid
bed temperature	70 C	for polylactic acid
adhesion type	brim	20 lines
stitching	keep open faces	disables stitching

The casting mold assembly (Figure 8) includes the aluminum base part, which has the same shape as the shear boxes in the portable shear box machine, and two plexiglass plates, which are connected to the both sides of the mold (Figure 9a). When using such molds traditionally, the shear surfaces of the core samples are upwards and the aluminum mold is at the bottom. In this project, the part of the mold which defines the topography of the shear surface is placed to the bottom and the aluminum mold is on the top of it. The aim of this method is to prevent the air bubbles in the concrete from sticking to the surface defining the topography. The air is obviously floating up in the wet concrete, therefore the bottom is the best possible place for the surface. Due to this method, the aluminum mold had to be modified so that casting would be possible when the aluminum mold is upside down. Therefore, approximately 5 cm x 2.5 cm hole was drilled to the bottom of the aluminum mold to enable casting through it (Figure 9b). The triangular bottom prism may be placed back to continue normal usage.

Laser cut plywood collar was used to house the 3D printed negative casting mold. The outer dimensions are 218 mm x 138 mm x 19.5 mm and the opening is 180 mm x 70 mm. The collars are coated with lacquer to prevent the concrete from sticking on it. The collar fits exactly between the protrusions and restrains the printed part in the right position. Thick grease is used between the aluminium mold and the frame and between the frame and the surface mold to improve water tightness.

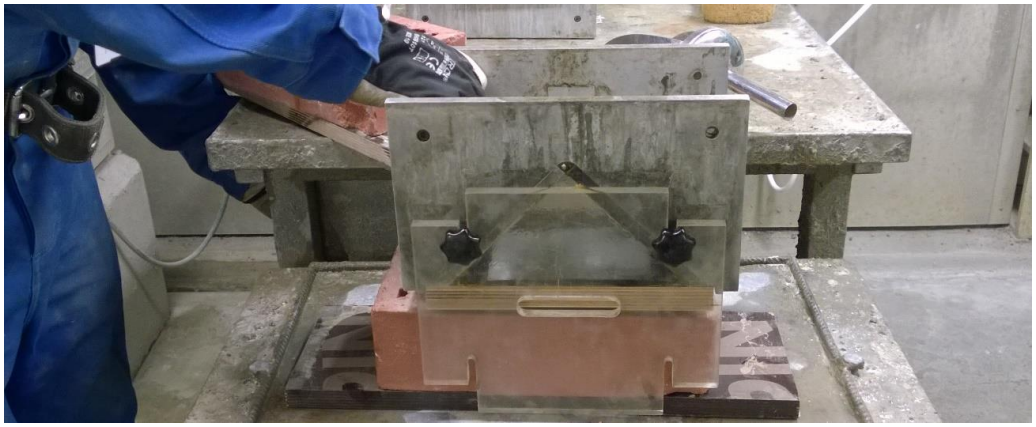

Figure 8. The entire casting mold assembly on top of a vibration table

Figure 9a. The aluminum mold with the plexiglass plates. Figure 9b. The casting hole drilled in bottom.

Replica production

Before casting, the plastic surfaces of the prototype mold were oiled with form oil to reduce adhesion to the concrete. Before the actual testing series was casted, the casting method was tested with the two pilot samples. The surfaces of the test samples were downscaled from the natural size using ratio 5:1. The aim was to investigate if air bubbles will stick to the plastic bottom of the mold and therefore make holes to the shear surface and potentially influencing the shear strength by acting as damage initiation areas.

The castings were performed with JB 1000/3 grouting mortar which has a strength class of C60/75-4 and a maximum grain size of 4 mm. The dry materials were applied first and then the water in small doses during the first three minutes of the total four minute mixing time. 3.1 liters of water were used per each 25 kg bag of ready-made mix, which results in water to cement ratio of 0.34. When casting the samples, both the bottom and top concrete always come from the same mixing batch. A waiting time of 20 min (24 min age) was used to reduce the swelling effect of the selected ready-mix mortar. The casting of the second mold typically began at 34 min age. The properties of the used mortar are shown in Table 3.

During the casting the entire assembly was vibrated extensively using a vibration table. 3 half scoops were enough to fill the replica surface to the collar top. After a short vibration to spread the mortar, the first long vibration took 30 seconds and the aim with that was to get all air bubbles out from the bottom plastic surface. After that, the mass was vibrated typically 8-10 times, 2-3 seconds at the time, to spread it evenly over the mold. At the end of the casting, one more 30 seconds vibration was done to release air bubbles from the mass. After casting, the samples were tightly sealed with a plastic bag to prevent the escape of moisture from the vicinity of the concrete. After 24 h storing, the molds were dismantled, the surfaces were inspected (Figure 10) and the replicas were moved into water immersion (18…22 C) for further curing. At the age of 7 days, the replicas were surface dried and tested with the portable shear box equipment.

Table 3. Properties of JB 1000/3 ready-made mix

Parameter	Value	Notes
strength class	C60/75-4	EN 206-1
compressive strength	45 MPa 1 d 70 MPa 7 d 90 MPa 28 d	+20 °C, EN 12190
binder	CEM II A 42.5 R	EN 206-1
water to cement	0.34	3.1 L water / 25 kg bag
aggregate size	0-4 mm	

Figure 10. Example of top surface quality of sample 1x14T with dimensions of 170 mm x 60 mm.

TESTING

Shear box tests were performed using the portable shear box machine. The equipment includes two aluminum halves of the shear box, a constant pressure pump for generating normal stress and a manual pump for generating shear force. The horizontal and vertical displacements are measured with dial gauges. The shear pressure values are read manually, but are also recorded on video for post-test checking.

The pressure is transmitted from the pumps to cylinders using oil. The hydraulic hose from the normal pressure pump to the normal force cylinder is particularly thick and stiff. Therefore, the shear box must be placed carefully with relation to the pump to avoid the hydraulic hose affecting any unwanted movement to the upper part of the shear box. The head of the normal force cylinder is against the cable loop whose other ends are fastened to the lower part of the shear box and vice versa. The cable loops are slightly flexible allowing the natural leaning of the shear surfaces upper part during the shear test. This also enables the measuring of the dilatation (Ross-Brown & Walton 1975).

The testing procedure follows the ISRM suggested method (Franklin et. al 1974) with the following exceptions: The matedness was checked using a powerful flashlight from the different edges around the sample. Connecting lines are drawn across the joint surface after the sample has been aligned. A normal pressure of 0.5 MPa was applied first and it remains constant during the test and the area loss will be compensated when analyzing the results. The effect of the stiffness of the shear piston assembly was measured to be 0.006 MPa/mm over the range of 0 mm to 20 mm. The effect of the shear assembly slack was measured to be 0.27 MPa and thus 0.5 MPa was chosen to be used as the initial shear for all samples. Shearing was performed up to 4 mm displacement. Shearing speed was 0.1 mm / min. The values of the shear pressure were logged at the beginning at points 0.025 mm, 0.050 mm, 0.075 mm and 0.100 mm. After this, the values were logged after each 0.1 mm displacements. The values of the shear pressure are read from the dial of the shear pressure pump. The reading accuracy of this logging method is approximately 0.05 MPa.

PILOT RESULTS

Pilot #0 was conducted in conjunction with the bachelor thesis of Raphaël Yorke and a joint surface was successfully replicated from a 50 mm core sample. Pilot #1 used synthetic geometry which was successfully printed and cast into concrete, but not shear tested. Pilot sample #2 used 625 mm x

575 mm (5:1) geometry from the center of the slab. It was replicated to a 125 mm x 115 mm sample. The pilot #3 used 170 mm x 60 mm (1:1) geometry and 170 mm x 60 mm sample size. The shear testing results are shown in Figure 11. In both experiments sudden spurts of movement occurred. This effect was more pronounced with the pilot #3 sample resulting in regions with no data. Pilot #2 reaches its peak shear stress of 0.64 MPa at 2.2 mm and pilot #3 reaches its peak load of 0.71 MPa at 1.5 mm. This indicates that smaller scales of asperities are active in the shearing of pilot #3.

The pilots show that the chosen concrete mix was strong enough and no significant abrasion of the surface occurred during the shearing. Some localized damage occurred at shearing direction in front edge of the shear surface (Figures 12 & 13). The failure occurred approximately in 60 degree angle downwards from the shear plane (Figures 14 & 15).

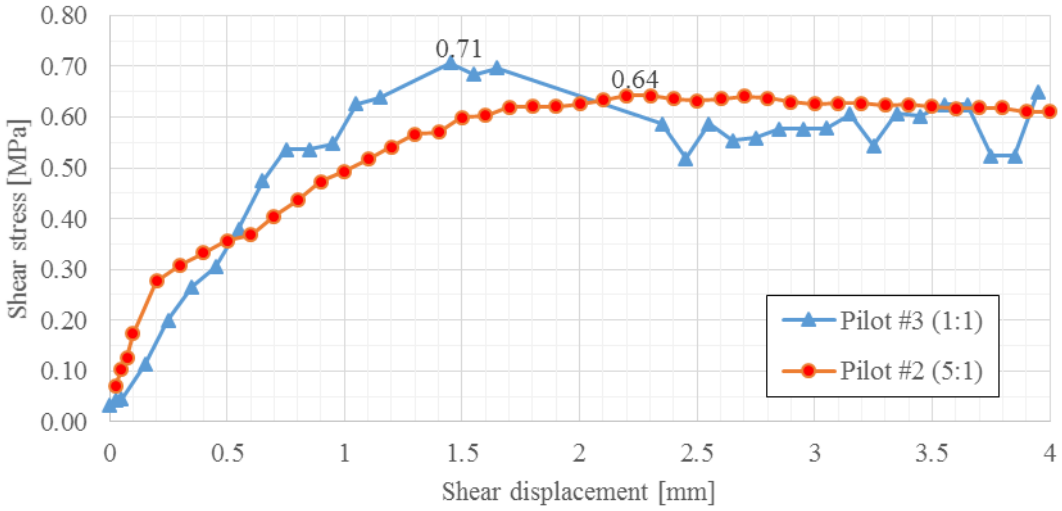

Figure 11. The shear stress – displacement curve of the pilot #2 and pilot #3

Figure 12. Pilot #2 bottom and top samples after loading


Figure 13. Pilot #3 sample top and bottom samples after loading

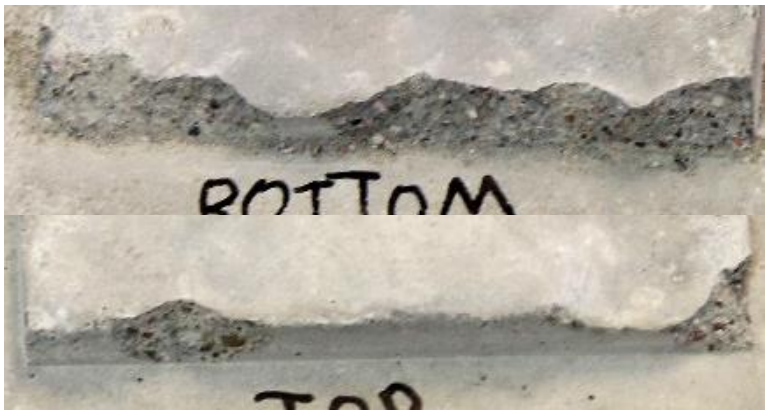

Figure 14. Closeup of the damaged front of pilot #2


Figure 15. Closeup of the damaged front of pilot #3

DISCUSSION

It could be discussed why to go through all this trouble of digital replication and 3D fabrication when the large joints could just be tested and then repeatedly sawed to smaller pieces and retested? Or why not just replicate using silicone putty if repeatability with concrete replicas is desired? Our method has two big advantages, it offers arbitrary control of scale without any abrasion effects related to retesting. Using silicone putty might be difficult if the surface to be replicated is large, but poses little challenge to optical methods of capturing the geometry.

If we manage to quantify the loss of geometry due to downscaling, the next step is to try to compensate for it. Then a large surface could be digitally subsampled, replica tested in small scale and then upsampled again producing the numerical modelling parameters for the (perfectly mated) larger joint surface. The validity of such upscaling could be verified by predicting the Tilt Table test properties of medium size laboratory samples from subsampled replicated geometry.

While high strength concrete seems to produce shear box results which are in the same order of magnitude with the actual rock samples, concrete is not rock and a matching series of actual rock joint samples and concrete replicas is needed to detect any systematic bias. Such testing campaign is planned in the upcoming continuation research programme.

CONCLUSIONS

The presented method is able to produce high density (e.g. 16.2 pts/mm^2) geometrical data using off-the-shelf photographic equipment and free software. Conventional modelling software may not be able to handle the resulting point cloud and the developed Python code may be used instead. The existing casting molds can be modified and used in combination with laser cut plywood collar and 3D printed replica molds. For rough joints, the accuracy of the replication is sufficient (20 layers per millimeter). The concrete reproduces the printed shape well (layer lines still visible), but air bubbles may cause problems and great care must be taken to vibrate the casts and to limit air content.

The replication method appears feasible, but not enough samples have been tested yet to draw conclusions based on the shear testing results. The pilots #2 and #3 do show the expected behavior: for larger geometries, the curve is smoother and doesn't have a clear peak point while the curve for smaller scale sample is more irregular and reaches its peak load at 1.5 mm displacement (Figure 11). We conclude that more testing is required to judge the true usability of this method.

ACKNOWLEDGEMENTS

This research project was funded by the Finnish Research Programme on Nuclear Waste Management KYT2014. Karri Mäkinen and Johanna Tikkanen are thanked for their help in improving the workability and surface quality of the concrete replica samples. Antoni Kopaly, Daniil Iakovlev and Stepan Kodeda are noted for their contribution in the manufacturing of the pilots and the primary testing series. Pekka Eloranta and Otto Hedström are thanked for their technical advice with the Portable Shear Box equipment. Meng Wang and Aalto ADDLAB are thanked for technical advice with 3D laser cutting technology and with 3D fused filament technology.

REFERENCES

Bandis, S.; Lumsden, A.C. & Barton, N.R. (1981) Experimental studies of scale effects on the shear behaviour of rock joints. Int J Rock Mech Min Sci & Geomech Abstr 18(1):1-21

Barton, N. & Choubey, V. (1977). The shear strength of rock joints in theory and practice. Rock Mechanics. Vol. 10:1-2. S. 1-54

Delaunay, B. (1934) Sur la sphère vide. Bulletin of the Academy of Sciences of the U.S.S.R. Classe des Sciences Mathématiques et Naturelle, Series 7 (6), 793-800

Dimitrov, D. (2008) Geometric Applications of Principal Component Analysis, Doctoral Dissertation, Institut für Informatik, Freie Universität Berlin, Germany

Franklin, J. A.; Kanji, M. A.; Herget, G. and Ladanyi, B.; Drozd, K. and Dvorak, A.; Egger, P.; Kutter, H.and Rummel, F.; Rengers, N.; Nose, M.; Thiel, K.; Peres Rodrigues, F. and Serafim, J. L.; Bieniawski, Z. T. and Stacey, T. R.; Muzas, F.; Gibson, R. E. and Hobbs, N. B.; Coulson, J. H.; Deere, D. U.; Dodds, R. K.; Dutro, H. B.; Kuhn, A. K. and Underwood, L. B. (1974) Suggested Methods for Determining Shear Strength, International Society for Rock Mechanics Commission on Standardization of Laboratory and Field Tests, Document No. 1

Girardeau-Montaut, D. (2012a) Girardeau, Cloud Compare manual: Transformation. Retrieved from: http://www.danielgm.net/cc/doc/CCLib/html/struct_c_c_lib_1_1_point_projection_tools_1_1_transformation.html

Girardeau-Montaut, D. (2012b) Girardeau, Cloud Compare manual: Delaunay2dMesh. Retrieved from: http://www.danielgm.net/cc/doc/CCLib/html/class_c_c_lib_1_1_delaunay2d_mesh.html

Hencher, S.R.; Toy, J.P. & Lumsden, A.C. (1993) Scale-dependent shearstrength of rock joints. In: Pinto Da Cunha A (ed) Scale effects in rock masses 93; proceedings of the 2nd international workshop on scale effects in rock masses, Lisbon, Portugal, 25 June 1993. A.A. Balkema, Rotterdam, pp 233–240

Korpi, E. (2014 expected) Quantifying loss of geometrical features in downscaling of rock joint surfaces using shear box replica series, master's thesis, Aalto University, Espoo, Finland

Kutter, H.K. & Otto, F. (1990) Influence of parallel and cross-joints on shear behaviour of rock discontinuities. In: Barton N, Stephansson O (eds) Rock joints, Loen, Norway, 4–6 June 1990. A.A. Balkema, Rotterdam, pp 243–250

Ross-Brown, D.M. & Walton, G. (1975) A portable shear box for testing rock joints. Rock Mechanics. Vol. 7:3. S. 129–153

Tatone, T., Grasselli, G. (2013) An Investigation of Discontinuity Roughness Scale Dependency Using

Yorke, R. (2014) Replicating joint geometry using 3D technology, bachelor's thesis, Aalto University, Espoo, Finland